Statistics of weakly scattered radar em waves with application to multiple channel SAR

By Brian C. Barber

Defence Science and Technology Laboratory, Cyber and Information Systems Division, Porton Down, Salisbury, UK

Abstract

This paper describes a new derivation of the probability density function of the background electromagnetic scatterers in sets of images generated by a Multiple channel Synthetic Aperture Radar (MSAR) operating with a wide bandwidth and long wavelength so that the resolution cell size is less than the mean wavelength. In such a situation the phase of the probability density function of the resultant of the scatterers may not be uniformly distributed over 2π. Moreover, the resultant of the scatterers may be correlated from channel to channel. The focus of interest is primarily the sea surface where the scatterers may be regarded as K distributed. A full analysis of the detection problem involves analysing a correlated non-isotropic 2D random walk where the 'steps' have a multivariate spherically invariant (non-Gaussian) distribution with a general coherence function and a non-uniform phase distribution. In this work the analysis is greatly simplified by considering limiting cases and exploiting physical arguments to simplify the analysis to the point where it becomes relatively straightforward. Examples are presented and it is found that there is an interesting choice of parameters where the radar is operated at a large grazing angle to give approximate Rayleigh scattering using a long wavelength and wide bandwidth giving a small degree of phase non-uniformity. In addition the time interval between the MSAR channels needs to be long enough so that the signals from the background scatterers are largely decorrelated from channel to channel. In this situation the theory indicates that coherent targets normally 'buried' in the clutter on the sea surface (including those targets casting a radar shadow) might be rendered more detectable.

1. Introduction

MSAR (Multiple channel Synthetic Aperture Radar) has the potential to detect and indicate slowly moving stealthy targets with high spatial resolution in difficult clutter. For example the detection and recognition of low radar scatter cross-section maritime targets such as small boats (especially for surveillance purposes) is an old problem but one which still presents many challenges. One major technical difficulty arises from the nature of the background clutter. Breaking waves can easily give scatter cross-sections comparable with the cross-section of a small target, especially a stealthy one. This paper discusses some theoretical statistical aspects of just one of the methods of dealing with this problem: the MSAR.

MSAR systems have active array antennas with panels which can be divided into sub-panels to give N multiple beams arranged along the track of the moving platform. In a typical arrangement one antenna beam is used to transmit and illuminate the target and then all of the antenna beams are used to receive the signals scattered from the target as the platform moves past the target. A set of N complex valued images is then processed using synthetic aperture techniques from the signals from each sub-panel and the images are registered and phase errors corrected. The images are weighted by a complex valued steering vector and linearly combined to produce a filtered image in which selected moving targets are enhanced relative to the background – see Barber & Barker (2012).

The radar beams are arranged along track and therefore there is a small time difference (typically milliseconds) between the signal data sets from each beam and therefore between each image. Hence when a target has a velocity component in the range direction of the radar there is a small change in range between each image and therefore a small phase change. In Barber & Barker (2012) generalised eigensystem theory is used to prove that for a perfectly coherent target the ratio of the target intensity to the mean background intensity is maximised when the weighting vector is a Fourier transform. The Fourier transform rotates the target image for each of the images so that the complex vectors 'line up' in the coherent sum so that the resultant is a maximum. It is shown that, for a perfectly coherent target, this maximises the target to background intensity ratio regardless of the statistical properties of the background. For the background only the existence of a coherence function is assumed and therefore the result is in general applicable to backgrounds having a 'spherically invariant distribution' such as the K distribution discussed in this paper.

An important consideration is what radar wavelength to use for such a radar. The scattering of coherent radar electromagnetic (e-m) waves from extended objects usually leads to signals having phases uniformly distrbuted over 2π. This is a consequence of typical radar waves having wavelengths much shorter than scattering scale lengths and resolution scales. However, for various reasons there has been a steady trend to longer radar wavelengths and also to

resolution scales comparable with wavelengths, especially in synthetic aperture radars. For a radar with a centre frequency of f_0 the maximum possible bandwidth is $2f_0$ leading to a maximum possible conventional resolution of $c/4f_0$ or $\lambda_0/4$. Such resolutions have been approached in recent experimental ultra wide bandwidth systems but an achievable and realistic figure for the resolution would be $\lambda_0/3$ for a radar operating in the VHF and UHF bands. This leads to a need to reconsider the statistical properties of *weakly* scattered e-m waves for radar backscatter because the resolution cell size is much smaller than the mean wavelength.

A full analysis of the detection problem involves analysing a correlated non-isotropic 2D random walk where the 'steps' have a multivariate spherically invariant (non-Gaussian) distribution with a general coherence function and a non-uniform phase distribution. This is a formidable undertaking and, although some progress is being made on this problem, in this work the analysis is greatly simplified by considering limiting cases and exploiting physical arguments to simplify the analysis to the point where it becomes straightforward. This paper considers only the probability density function of the background the complete detection problem is left for a future paper.

Since the simple steering vector described above maximises the target to background mean intensity ratio it will also necessarily maximise the detection probability for a given (perfectly coherent) target, background probability distribution *and radar system*. There is however an important consideration in the design of the radar system and this depends on two time scales. These are the decorrelation time of the scatterers (or the temporal coherence time) and the time difference between the images in the MSAR set (called here the interferometer time). The coherence time of the background t_c is on the order of the inverse of the Doppler bandwidth of the scattered radar signals and the interferometer time t_i is on the order of the distance between successive antenna sub-panels divided by the speed of the platform. An important consideration in the design of a MSAR system is the relative magnitude of t_c and t_i. This paper develops the work described in Barber & Barker (2012) by considering some theoretical aspects of the moments of the background scattering for two cases: (i) $t_c > N t_i$, and (ii) $t_c < t_i$. These cases are considered for ultra wideband systems where the resolution cell size is smaller than the centre wavelength of the radar.

2. The probability density functions for cases (i) and (ii)

This is a complex problem and in order to develop a tractable analysis some simplifying assumptions need to be made which nevertheless, as usual, retain the essential physics of the problem. To this end only the two limiting cases of $t_c > N t_i$ and $t_c < t_i$ are analysed here.

The addition of N complex valued images leads to an $N-$step random walk. The scattering of coherent radar electromagnetic (e-m) waves from extended moving objects like the sea surface usually leads to signals having phases uniformly distrbuted over 2π (*strong* scattering). This is a consequence of typical radar waves having wavelengths much shorter than scattering scale lengths and resolution scales. However in this case the important phases are not the 'absolute phases' of the scatterers but the phase *differences* between the resultants of the background scatterers contained in a radar resolution cell from image to image in the MSAR set of N images. When the images are correlated (because the scatterers are correlated) the phase difference will generally be less than 2π. In addition, because the resolution cell size is assumed smaller than a wavelength these phase differences will again be significantly less than 2π. Both these effects lead to phases not uniformly distributed over 2π.

Case (i): $t_c > N t_i$

In this case the coherence time of the scatterers is assumed to be greater than the total interferometer time of the MSAR. Suppose that each resolution cell in each image contains the resultant of n scatterers (a large number). Further, because $t_c > N t_i$ these same scatterers will be present in each of the N images contained in the MSAR image set. It is therefore assumed that because $t_c > N t_i$ and essentially the *same* scatterers are present in all of the images this leads to the amplitudes of the scattered waves being essentially the same in each of the images in the MSAR image set. For perfectly stationary scatterers the phase shift from image to image in the MSAR set will be zero. However, in the case of the sea surface the scatterers are not stationary and have speeds with both a random component and a directed component some moving towards the radar and some away from the radar. In addition, the phase rotation applied to the target in order to maximise the target image intensity is also applied to the background scatterers. It is therefore assumed that the net effect will then be to give, on average, a small non-uniformity in the phase distribution of the phase shift from image to image of each scatterer in each resolution cell. Then the phase difference between the images of the scatterers in each resolution cell will be less than 2π. Therefore the resultant of n e-m waves in a resolution cell

scattered from an object (such as the sea surface) over N images is modelled as the resultant of a random walk with the e-m waves scattered from each scatterer having a phase distribution not uniform over 2π.

In this case, therefore, it is assumed that the amplitudes of the waves remain the same from image to image but the phases of the waves are assumed statistically independent and have a von Mises phase distribution. This model captures the phase non-uniformity whilst giving a straightforward analysis. The pdf of the resultant of an nN step (n scatterers and N images) random walk where the amplitude of the steps (waves) is constant but the phases fluctuate with a von Mises distribution is given by:

$$p(a,\theta) = a\frac{\exp(\rho a\cos\theta)}{2\pi}\left[\frac{1}{\mathrm{I}_0(\rho r)}\right]^{nN}\int_0^\infty\left[\mathrm{J}_0(\alpha r)\right]^{nN}\mathrm{J}_0(\alpha a)\,\alpha\,\mathrm{d}\alpha \qquad (2.1)$$

see Barber (1993), §6.2. I_0 and J_0 have their usual Bessel funtion meaning, a is the resultant of the walk (ie the amplitude of the random sum of the waves), r is the length of each step (this represents the root mean square amplitude of each of the scattered waves assumed the same for a uniform scatterer), θ is the phase of the resultant and ρ ($\rho \geq 0$) is a parameter determining the non-uniformity of the phase. When $\rho = 0$ the scattering is strong (phase distribution uniform over 2π) and as ρ becomes large the phase becomes more and more non-uniform until the walk becomes essentially one dimensional. All processes are assumed stationary.

For a large number of scatterers (ie large n):

$$\left[\mathrm{I}_0(\rho r)\right]^{-nN} \approx \exp\left(-nN\rho^2 r^2/4\right) \quad \text{and} \quad \left[\mathrm{J}_0(\alpha r)\right]^{nN} \approx \exp\left(-nN\alpha^2 r^2/4\right) \qquad (2.2)$$

see Watson (1952), §13.48. Hence:

$$p(a,\theta) \approx \frac{2a}{N\langle I\rangle}.\frac{\exp(\rho a\cos\theta)}{2\pi}.\exp\left[-\frac{\rho^2 N\langle I\rangle}{4}-\frac{a^2}{N\langle I\rangle}\right] \qquad (2.3)$$

where $\langle I\rangle = nr^2$ and represents the total 'mean intensity' of the scatterers.

Radar scattering is usually non-Gaussian, and this is especially true for scattering from the sea surface at small to moderate grazing angles – see Ward, Tough & Watts (2012). In radar modelling, especially of sea surface scattering, it is often assumed that the local mean is a fluctuating quantity (Ward et al 2012, Jakeman & Tough 1988). The mean intensity is taken to be uniform within a resolution cell but over a number of cells it can fluctuate. This can be justified on the basis of experimental results (Ward et al 2012) or as a consequence of the scatterers undergoing a birth-death-immigration process (Jakeman & Tough 1988), or on the basis of an argument based on a statistical mechanical analogue (Lienhard & Meyer 1967). In consequence of the above referenced work, the fluctuations of mean intensity (the 'envelope' of the modulation) are here taken to have a gamma distribution. The pdf given above in (2.3) can be viewed as being conditional on $\langle I\rangle$ and the fluctuations can then be accomodated by simply compounding (2.3) with a gamma distribution. Another way of looking at this is on the basis of a mixture of pdfs given by (2.3) with $\langle I\rangle$ scaled by a gamma distribution to give a 'scale mixture distribution'. This technique then gives the required non-Gaussian (K) distribution with relatively 'fat tails'. Because the amplitudes of the scattered waves are essentially the same for the corresponding resolution cells in the each image in the MSAR set the scaling can be carried out on the resultant of the random walk just as well as on each individual component wave in the walk since the scaling just magnifies or attenuates the scale of the walk in this case. The phases do change from image to image however. As discussed above the phase rotation applied to the target to maximise the target intensity is also applied to the background scattered waves and also the scatterers are located at slightly different ranges within the resolution cell. Thus in the limit $t_c > N t_i$ the physics can be exploited so as to make the analysis tractable. Let the fluctuations in mean intensity have a gamma distribution then:

$$p\left(\langle I\rangle\right) = b^{\upsilon}\langle I\rangle^{\upsilon-1}\exp\left(-b\langle I\rangle\right)\Big/\Gamma(\upsilon) \qquad (2.4)$$

The parameter b ($b \geq 0$) is essentially a scale, and υ ($\upsilon > 0$) is a 'shape' parameter. Scaling (2.3) on the basis of (2.4) and then integrating over θ to give the marginal pdf for a gives:

$$p(a)=\frac{4b^{\upsilon}a^{\upsilon}}{N\Gamma(\upsilon)(N\eta)^{(\upsilon-1)/2}}\mathrm{I}_0(\rho a)\mathrm{K}_{\upsilon-1}\left(2a\sqrt{\eta/N}\right) \qquad (2.5)$$

where $\eta=b+N\rho^2/4$. Compare with equation 2.29 of Jakeman & Tough (1988) where a similar result is obtained (for $N=1$) using different methods. The case $\rho=0$ corresponds to strong scattering and a uniform phase distribution and then a K distribution results:

$$p(a)=\frac{4a^{\upsilon}}{\Gamma(\upsilon)}\left(\frac{\mathrm{b}}{\mathrm{N}}\right)^{(\upsilon+1)/2}\mathrm{K}_{\upsilon-1}\left(2a\sqrt{b/N}\right) \qquad (2.6)$$

in agreement with equation 4.25 of Ward et al (2012) when $N=1$. The case of ρ small rather than zero is the case of most interest here. On the other hand when ρ is large it can be shown that (2.5) becomes a gamma distribution. This is to be expected since when ρ is large the underlying random walk becomes one dimensional and this reflects the assumed gamma distribution for the mean intensity given in equation (2.4). However, this particular case is not relevant for the problem under consideration here.

The m^{th} moment of the resultant given by (2.5) is

$$\left\langle a^m\right\rangle=\left(1-\frac{N\rho^2}{4\eta}\right)^{\upsilon}\left(\frac{N}{\eta}\right)^{m/2}\frac{\Gamma(\upsilon+m/2)\Gamma(1+m/2)}{\Gamma(\upsilon)}\,{}_2F_1\left(\upsilon+m/2,1+m/2;1;N\rho^2/4\eta\right) \qquad (2.7)$$

see Erdelyi et al (1953), §7.14.2 (35). Put $m=0$ then $\langle 1\rangle=1$ since ${}_2F_1\left(\upsilon,1;1;N\rho^2/4\eta\right)=\left(1-N\rho^2/4\eta\right)^{-\upsilon}$.

Case (ii): $t_c<t_i$

In this case the background scatterers are mostly decorrelated from image to image in the interferometer set. Hence one can view the individual images as containing *different* scatterers and *different* scattered waves. Again it is assumed that the scatterers undergo a modulation process as described above in case (i) leading to a K distribution. Because the resolution cell size is assumed significantly less than the mean wavelength of the radar the phase will be non-uniform and therefore the phase difference of the resultant of the waves for a given resolution cell from image to image in the MSAR set will be on average less than 2π despite the scatterers being essentially not physically correlated. In this case it is assumed that in the underlying random walk each of the n scattered waves from the background in each image is itself K distributed with a small non-uniform phase distribution over 2π. The von Mises distribution is again used as a model for analytic convenience. The pdf of the resultant of such a walk is given in Barber (1993), §6.3. Suppose that the pdf for the k^{th} wave is:

$$p_k(r_k)=\beta r_k^{\upsilon+1}\frac{\exp(\rho r_k\cos\phi_k)}{2\pi}\mathrm{K}_{\upsilon}(\eta r_k) \qquad (2.8)$$

where β is a normalising constant

$$\beta=\left(\eta^2-\rho^2\right)^{\upsilon+1}\Big/(2\eta)^{\upsilon}\,\Gamma(\upsilon+1) \qquad (2.9)$$

The pdf of the modulus of the resultant of N images of the background is then

$$p(a)=\left[\frac{a\left(\eta^2-\rho^2\right)}{2\eta}\right]^{N(1+\upsilon)}\frac{2\eta}{\Gamma\left[N(1+\upsilon)\right]}\mathrm{I}_0(\rho a)\mathrm{K}_{N(1+\upsilon)-1}\left(N(1+\upsilon)a\right) \qquad (2.10)$$

The m^{th} moment of the resultant is given by

$$\left\langle a^m \right\rangle = \left(1-\frac{\rho^2}{\eta^2}\right)^{\mu+1}\left(\frac{2}{\eta}\right)^m \frac{\Gamma\left(1+\mu+m/2\right)\Gamma\left(1+m/2\right)}{\Gamma\left(1+\mu\right)}\,{}_2F_1\left(1+\mu+m/2,1+m;1;\rho^2/\eta^2\right) \qquad (2.11)$$

where $\mu = N\left(1+\upsilon\right)$. See Erdelyi et al (1953), §7.14.2 (35). Put $m=0$ then $\left\langle 1\right\rangle = 1$ since ${}_2F_1\left\{1+\mu,1;1;\rho^2/\eta^2\right\} = \left(1-\rho^2/\eta^2\right)^{-(\mu+1)}$.

3. Examples and discussion.

There are many parameters in this problem and an exhaustive survey of the properties of (2.5), (2.7), (2.10) and (2.11) is not possible here. However, eight examples are presented which, it is hoped, give an idea of the possibilites of the MSAR in the two cases discussed above. In all the examples the scale factor b is set to one. Also only a four beam MSAR is considered so that $N=4$. This value of N is large enough to show the effects of combining images in an MSAR but small enough to be a feasible engineering proposition. The examples are shown in figures 1-4. Table 1 lists the examples illustrated by the figures.

Figure	Case	υ	ρ
1	(i)	1	0.0
1	(i)	1	0.1
2	(i)	100	0.0
2	(i)	100	0.1
3	(ii)	1	0.0
3	(ii)	1	0.1
4	(ii)	100	0.0
4	(ii)	100	0.1

TABLE 1. List of the υ and ρ parameters presented for cases (i) and (ii) in figures 1,2,3 and 4

When $\upsilon \to \infty$ the K distribution tends to the Rayleigh distribution (see Ward et al 2012) and a value of $\upsilon = 100$ was chosen to illustrate this. On the other hand small values of υ led to 'spiky' scatterer behaviour with the resulting K distribution having 'fat tails'. This situation is illustrated by $\upsilon = 1$. The phase non-uniformity is set by the ρ parameter and the case of uniform phase distribution over 2π corresponds to $\rho = 0$. A small degree of non-uniformity is given by $\rho = 0.1$ and both $\rho = 0.1$ and $\rho = 0$ are illustrated in figures 1-4. In the case of sea surface scattering (the situation of interest here) the magnitude of υ depends very much on the grazing angle of the radar. Small grazing angles (roughly 1º or less) tend to give small values of υ (less than 1). On the other hand large grazing angles (roughly greater than 45º give approximately Rayleigh scattering with υ large (100 or more). Discounting any operational constraints the magnitude of υ can be selected on the basis of grazing angle.

Case (i): $t_c > N t_i$

In the first example for case (i) corresponding to $\upsilon = 1$, the mean of the pdf is roughly doubled by the phase non-uniformity whereas the shape of the pdf remains roughly the same. This is shown in figure 1. The coherent addition of the target as explained in Barber & Barker (2012) will increase the mean of a coherent target by four times for a four channel MSAR and this will be the same for both $\rho = 0$ and $\rho = 0.1$. In this example therefore the detection performance will be degraded by the phase non-uniformity for a coherent target.

In the second example for case (i), again for $t_c > N t_i$, but now $\upsilon = 100$, illustrates that the mean of the pdf for the background is increased by over an order of magnitude for a small phase non-uniformity. This is shown in figure 2. The same argument applies as in the case of the previous example only to a greater degree. For the Rayleigh situation with large υ the detection performance will be severely degraded by the phase non-uniformity.

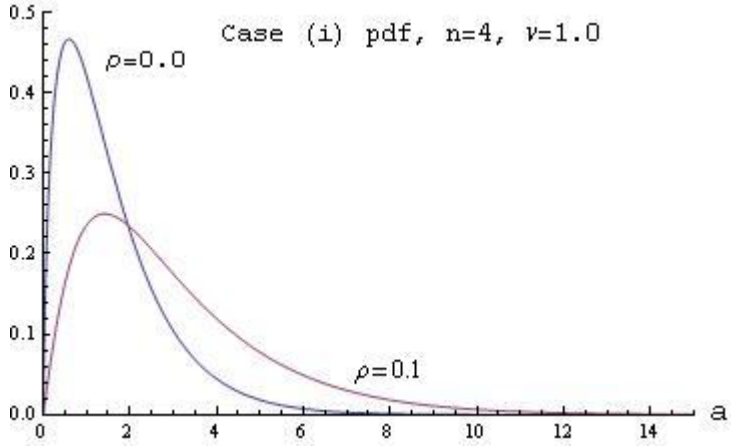

FIGURE 1. Probability density functions for case (i) for $N=4$, $b=1$ and $\upsilon=1$.

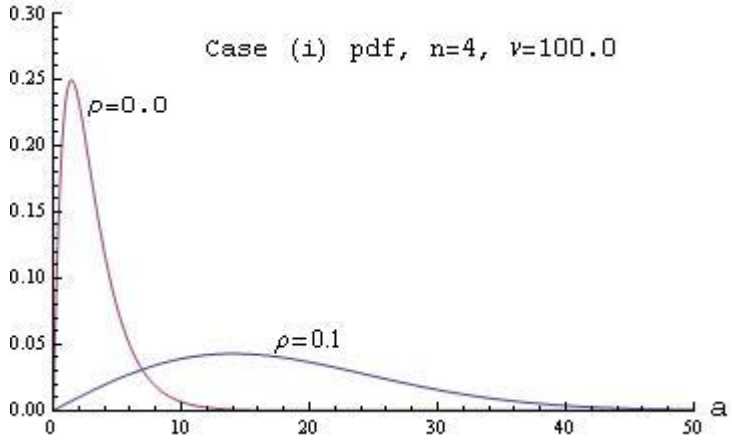

FIGURE 2. Probability density functions for case (i) for $N=4$, $b=1$ and $\upsilon=100$.

Case (ii): $t_c < t_i$

In the first example for case (ii) corresponding to $\upsilon=1$, shown in figure 3, both the mean and the shape of the pdf are hardly changed by the phase non-uniformity. As a result the detection performance for a coherent target in a simple binary detection hypothesis situation is very insensitive to small amounts of phase non-uniformity.

The pdf for the second example for case (ii), again for $t_c < t_i$, but now $\upsilon=100$, is shown in figure 4. This example is the most interesting of the four presented here. In this example $t_c < t_i$ as in the previous one but the scattering is now more Rayleigh in character because υ is large. The mean of the pdf has increased roughly three times but the *shape of the pdf has changed* and is now is bell shaped. This has an interesting implication for the simple binary detection hypothesis scenario. The pdf of a weak target buried in the clutter will tend to be separated from the clutter pdf as the mean of the clutter pdf increases with the phase non-uniformity. It can be shown that the ratio of the standard deviation of the pdf to the mean becomes ever smaller as υ increases in this case. This example shows that low scatter cross-section targets might be detectable in principle by the MSAR technique when the system is designed so that $t_c < t_i$ and there is at least a small degree of phase non-uniformity. As pointed out in the Introduction this would correspond to a relatively long wavelength (and also to a relatively long time interval between the channels in the MSAR).

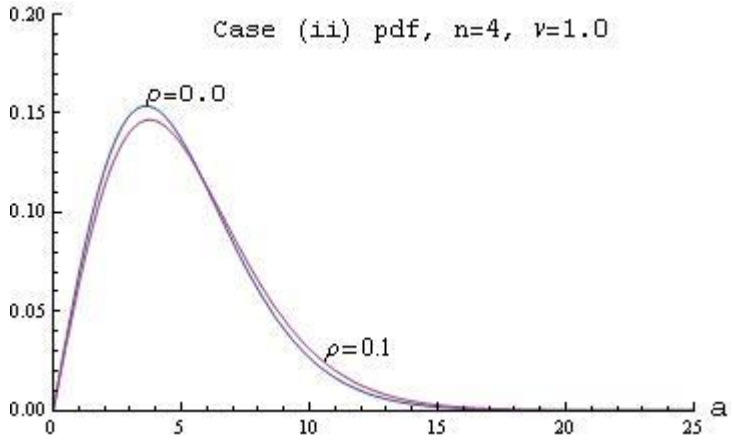

FIGURE 3. Probability density functions for case (ii) for $N=4$, $b=1$ and $\upsilon=1$.

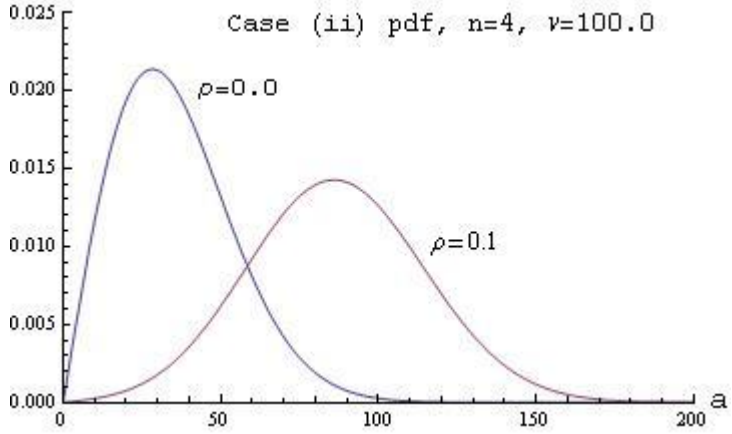

FIGURE 4. Probability density functions for case (ii) for $N=4$, $b=1$ and $\upsilon=100$.

Another class of targets which would be more detectable by operating an MSAR in this parameter space is the shadow target. In this situation a target gives a radar shadow due to the masking of physical scatterers. Clearly such a target would have a higher detection probability if the background can be processed to have a smaller ratio of standard deviation to mean.

4. Conclusion.

In this work a difficult and largely intractable problem in applied probability has been attacked by exploiting the physics to give a simplified analysis which nevertheless hopefully retains sufficient reality to render the work useful – time will tell. The work is of a preliminary nature and is ongoing. Nevertheless, there are interesting indications that by operating a multiple channel synthetic aperture radar in a specific parameter space the detection performance over a standard SAR can be improved for an important class of targets. In particular the radar should be operated at a large grazing angle to give Rayleigh scattering using a long wavelength and wide bandwidth to give a resolution less than the mean wavelength thus giving a small degree of phase non-uniformity. In addition the time interval between the MSAR channels needs to be long enough so that the signals from the background scatterers are largely decorrelated from channel to channel. In this situation the indications are that low cross-section targets normally 'buried' in the clutter on the sea surface (including those targets casting a radar shadow) might be rendered more detectable.

5. Acknowledgement.

This work was funded by the author's Fellowship of the Defence Technology and Science Laboratory, Ministry of Defence.

REFERENCES

BARBER, B. & BARKER, J. 2012. Indication of slowly moving ground targets in non-Gaussian clutter using multi-channel synthetic aperture radar. *IET Signal Processing* **6**, 424-434.

BARBER, B. C. 1993. The non-isotropic two-dimensional random walk. *Waves in Random Media* **3**, 243-256.

ERDELYI, A., MAGNUS, W., OBERHETTINGER, F. & TRICOMI, F. G. 1953. Higher Transcendental Functions vol. 2. McGraw-Hill.

JAKEMAN, E. & TOUGH, R. J. H. 1988. Non-Gaussian models for the statistics of scattered waves. *Advances in Physics* **37**, 471-529.

LIENHARD, J. H. & MEYER, P. L. 1967. A physical basis for the generalised gamma distribution. *Quarterly of Applied Mathematics* **25**, 330-334.

WARD, K. D., TOUGH, R. J. H. & WATTS, S. 2012. Sea Clutter: Scattering, the K Distribution and Radar Performance. 2nd Ed. IET.

WATSON, G. N. 1952. Theory of Bessel Functions. 2nd Ed. CUP.